Research Article | Vol. 13, No. 4 / 1 Apr 2022 / Biomedical Optics Express 2174
Biomedical Optics EXPRESS

Intraocular scatter compensation with spatial light amplitude modulation for improved vision in simulated cataractous eyes

SPOZMAI PANEZAI,[1] ALFONSO JIMÉNEZ-VILLAR,[1] ALBA M. PANIAGUA DIAZ,[2] AUGUSTO ARIAS,[2] GRZEGORZ GONDEK,[1] SILVESTRE MANZANERA,[2] PABLO ARTAL,[2] AND IRENEUSZ GRULKOWSKI[1,*]

[1]*Institute of Physics, Faculty of Physics, Astronomy and Informatics, Nicolaus Copernicus University in Toruń, ul. Grudziądzka 5, 87-100 Toruń, Poland*
[2]*Laboratorio de Óptica, Universidad de Murcia, Campus de Espinardo (Edificio 34), E-30100 Murcia, Spain*
[*]*igrulkowski@fizyka.umk.pl*

Abstract: Cataract is one of the common causes of visual impairment due to opacification of the crystalline lens. Increased intraocular scattering affects the vision of cataract patients by reducing the quality of the retinal image. In this study, an amplitude modulation-based scatter compensation (AM-SC) method is developed to minimize the impact of straylight on the retinal image. The performance of the AM-SC method was quantified by numerical simulations of point spread function and retinal images in the presence of different amounts of straylight. The approach was also experimentally realized in a single-pass system with a digital micro-mirror device used as a spatial amplitude modulator. We showed that the AM-SC method allows to enhance contrast sensitivity in the human eyes *in vivo* with induced scattering.

© 2022 Optica Publishing Group under the terms of the Optica Open Access Publishing Agreement

1. Introduction

Interaction of electromagnetic radiation with tissues give rise to scattering due to the heterogeneity of biological objects. The effect of scattering limits the performance of medical imaging modalities by reducing the quality of image reconstruction and quantitative analysis [1,2]. In particular, scattering reduces the penetration depth of light in tissues, being a fundamental challenge in optical imaging through turbid media. Several hardware and computational approaches have been developed to enable imaging through scattering layers and to increase the effective imaging depth [3–8].

The visual process starts with the image formation on the retina, which is mostly enabled by light refraction at the corneal and the crystalline lens interfaces. Light has to pass through the ocular structures (cornea, crystalline lens) and media (aqueous, vitreous) before reaching the retina. Consequently, optical aberrations and scattering, caused by pathological opacifications formed in any part of the light path within the eye globe affect the retinal image quality and therefore can reduce vision significantly [9].

Cataracts are a common condition of the eye, in which the crystalline lens become less transparent (more cloudy) due to the formation of opacifications. In particular, ageing and other factors, such as increased ultraviolet light exposure or diabetes etc. contribute to the development of crystalline lens opacities and give rise to the enhanced backward and forward intraocular scattering [10]. Cataracts are clinically diagnosed based on the observation of the backscattered light from the lens opacifications during slit lamp examination [11]. Recent developments in ophthalmic technologies, such as the double-pass techniques and optical coherence tomography, enable a more complete analysis of the crystalline lens opacities and a less subjective cataracts

#451878 https://doi.org/10.1364/BOE.451878
Journal © 2022 Received 22 Dec 2021; revised 7 Mar 2022; accepted 8 Mar 2022; published 16 Mar 2022

Biomedical Optics EXPRESS

evaluation [12–15]. In addition, cataract causes blurring and reduction of contrast of the retinal image [16]. The impact of cataract on vision function is tested clinically with visual acuity tests. Accordingly, it is forward scattering (straylight) that contributes to reduction of the quality of vision [17]. Currently, cataract treatment is only possible by surgery in which the crystalline lens is replaced by an intraocular lens implant [18]. However, cataract surgical intervention still represents challenges in some situations like congenital cataract in infants [19]. Therefore, non-invasive vision improvement approaches would be considered a beneficial complementary option in the cases of inoperable cataract or when one wants to avoid the risk of post-surgical complications.

Different optical engineering techniques have been proposed to compensate for the intraocular scattering and to reduce the effect of light scatter on the retinal image. Miller et al. used holography to retrieve and compensate the phase of an *ex vivo* cataractous lens [20]. Similarly, Liu et al. applied time-reversing optical phase conjugation to focus through an *ex vivo* cataractous lens [21]. Arias and Artal developed a feedback-based wavefront shaping technique via spatial light modulator to compensate the effect of scattering due to cataract and to improve the vision quality [17]. Recently, Paniagua-Díaz et al. demonstrated that point spread function (PSF) from retinal fluorescence signal (like retinal pigment epithelium fluorescence) along with wavefront shaping can be used for scatter compensation and potential vision improvement [22]. Finally, However, wavefront shaping for the optical compensation of lenticular opacities involves lengthy and precise calculations and optimization, which limits its practical application.

The aim of this study was to develop the method of spatial light amplitude modulation within the eye pupil to minimize the impact of opacities in the crystalline lens on the retinal image. We firstly investigate the performance of the proposed approach by numerical simulations considering eyes with different amounts of intraocular straylight, representative for early and advanced cataracts. Later, the approach was implemented experimentally with a Digital Micromirror Device (DMD) as amplitude pupil modulator in a single-pass system, and the performance of the method was assessed by a contrast sensitivity test in the human eyes *in vivo* with artificial light scatter model (cataract phantom).

2. Materials and methods

2.1. Amplitude modulation-based scatter compensation method (AM-SC)

The opacities of the crystalline lens impart scattering of light propagating through the eye, which results in blurring the retinal image (Fig. 1(a)). The amplitude modulation-based scatter compensation (AM-SC) methodology blocks the illumination of the lens opacifications, reducing deteriorating effects of the opacities on the retinal images. The proposed method aims at minimizing the impact of straylight on retinal image quality by spatial light modulation within the eye pupil. The AM-SC method is a two-step procedure that has been schematically presented in Fig. 1(b). The proposed approach involves the following stages:

a) Mapping of light scattering

AM-SC technique is based on a prior knowledge on the spatial distribution of opacified regions inside the pupil area. Therefore, light scattering has to be mapped with any optical imaging modality (e.g. optical coherence tomography, OCT). *En-face* projection of light scattering is represented by an opacity map that is later used to generate a complementary binary mask, as shown in Fig. 1(b).

b) Modulation of light intensity at the pupil plane by conjugated binary mask on spatial light modulator

A binary, amplitude mask is generated to block the light interacting with the opacities in the cataractous lens. Basically, this mask corresponds to the complement of the binarized map

Biomedical Optics EXPRESS

of opacities. The light is projected to the eye through a spatial amplitude modulator (e.g. a digital micro-mirror device, DMD) which is conjugated with the eye pupil. The mask is programmed in the modulator, expecting the improvement on the retinal image, as shown in Fig. 1(b).

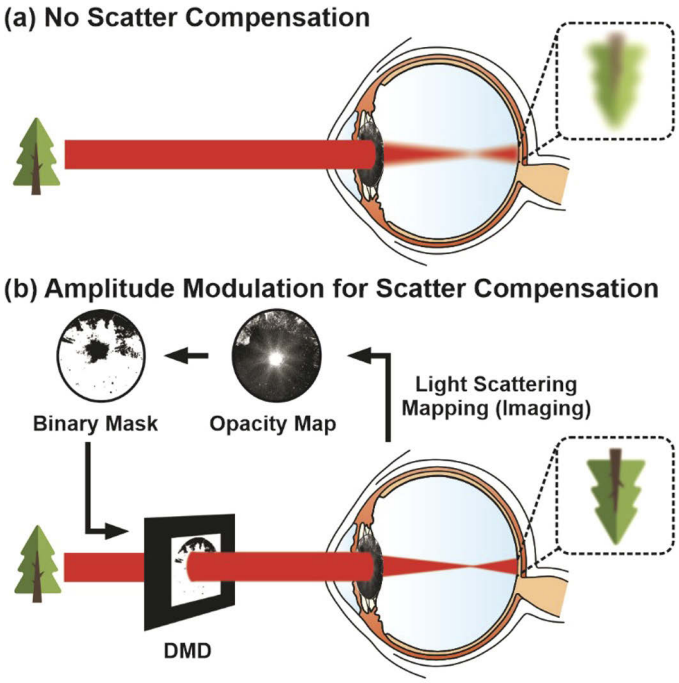

Fig. 1. Concept of the proposed amplitude modulation-based scatter compensation method in cataract eyes. (a) Opacification in the anterior segment of the eye results in reduced retinal image quality (blur, poor contrast). (b) Mapping intraocular light scattering allows for generation of the opacity map of the crystalline lens, which is later transformed into a binary mask. The light entering the eye is spatially modulated by a digital micro-mirror device (DMD) to allow the light to pass through non-opacified regions, which reduces the impact of intraocular scatter on vision.

The AM-SC methodology does not allow the light incident on the pupil to interact with the opacities as the opacified regions within the pupil are not illuminated. Hence, the intraocular scattering no longer plays significant role in deteriorating retinal PSF, and the retinal image blurring is reduced, which should result in vision improvement of a cataract patient.

2.2. Numerical simulations

The numerical simulations of different levels of straylight in cataract were performed to study the effect of opacities on the retinal image and to assess the performance of the AM-SC method. We modelled the effect of opacities, on the light beam propagating through the eye as random phase perturbations [23]. The wavefront $W(x_i, y_j)$ can be calculated using inverse discrete cosine transform (IDCT) of a standard normally distributed random numbers R weighted by a power law function P in spatial frequency domain:

$$W(x_i, y_j) = IDCT\{P(f_i, f_j)R(f_i, f_j)\} = \\ = \sum_{i=0}^{N-1}\sum_{j=0}^{N-1} P(f_i, f_j)R(f_i, f_j)\cos(\tfrac{\pi df_i}{N}x_i)\cos(\tfrac{\pi df_j}{N}y_j) \quad , \tag{1}$$

Biomedical Optics EXPRESS

where: f_i and f_j are the spatial frequencies of cosine modes in horizontal (x) and vertical directions (y), x_i and y_j are Cartesian coordinates and d is the diameter of the pupil, respectively. The functions $P(f_i, f_j)$ and $R(f_i, f_j)$ are represented by matrices of $N \times N$ ($N = 2000$ in all calculations). The power law function $P(f_i, f_j)$ presents the contribution of different spatial frequencies (angular profile of scattered light distribution) in the final phase map:

$$P(f) = Bf^{\beta}, \tag{2}$$

where: $f = \sqrt{f_i^2 + f_j^2}$ is the radial spatial frequency. The coefficients B and β were selected to simulate the point spread function in accordance to the criteria of the Commission International d'Eclairage (CIE) [24]. In the simulations, we took into account two levels of straylight described by $\mathrm{Log}_{10}(s) = 1.75$ and 2.37 (quantified at an angle of 6 degrees), which corresponded to nuclear cataracts of rank 3 or higher in the Lens Opacity Classification System III (LOCS III).

The light field perturbed by the opacification can be therefore described by:

$$E(x_i, y_j) = circ\left(\frac{r}{d}\right) \exp[W(x_i, y_j)], \tag{3}$$

where the amplitude is described by circ function (pupil):

$$circ\left(\frac{r}{d}\right) = \begin{cases} 1 & \frac{r}{d} \le \frac{1}{2} \\ 0 & otherwise \end{cases}, \tag{4}$$

where: d is the diameter of the pupil (= 2.7 mm in our simulations), and $r = \sqrt{x_i^2 + y_j^2}$ is the radial coordinate.

The point spread function (PSF) of the cataract eye was calculated by taking the fast Fourier transform of the light field:

$$PSF = |FFT\{E(x_i, y_j)\}|^2. \tag{5}$$

The retinal image I in the presence of intraocular scatter was then calculated by convolving the PSF with the projected ground truth image I_g:

$$I = PSF \otimes I_g. \tag{6}$$

In the simulations, the random phase spatial distribution $W(x_i, y_j)$ served as the opacity map. AM-SC method requires generation of binary mask based on opacity map. Accordingly, the phase map was converted to 8-bit map of unsigned integers (0-255) and thresholded so that pixels with values below 51 were zeroed out. To make the binary mask more realistic, additional steps of segmentation has been carried out by watershed transform method. Finally, the binary mask is inverted so that the transparent regions unaffected by opacification (lower signal in phase mask) were represented by values 1 in the array whereas opacified regions (higher signal in phase mask) corresponded to values 0.

To test the performance of AM-SC technique, the binary mask $M(x_i, y_j)$ was placed in front of the pupil so that element-wise multiplication of matrices were done to calculate the light field:

$$E_{AM-SC}(x_i, y_j) = E(x_i, y_j) \cdot M(x_i, y_j), \tag{7}$$

Analogously, the PSF of the cataract eye after applying AM-SC method was given by:

$$PSF_{AM-SC} = |FFT\{E_{AM-SC}(x_i, y_j)\}|^2. \tag{8}$$

The retinal image I_{AM-SC} compensated for scatters by AM-SC method was given by the formula:

$$I_{AM-SC} = PSF_{AM-SC} \otimes I_g. \tag{9}$$

The tests of the AM-SC method were conducted using synthetic ground truth images in the form of sine-wave gratings of variable spatial frequencies 2, 6, 12 and 20 cycles per degree

Biomedical Optics EXPRESS

(CPD), each with two contrast values: 100% (high contrast) and 50% (low contrast). Two amounts of straylight were simulated to show different cataract grades: $\mathrm{Log}_{10}(s) = 1.75$ and $\mathrm{Log}_{10}(s) = 2.37$, which corresponded to the following sets of coefficients B and β in Eq. (2): $B = 11.64\,\mu m$ and $\beta = -1.21$ for $\mathrm{Log}_{10}(s) = 1.75$, and $B = 24.17\,\mu m$ and $\beta = -1.21$ for $\mathrm{Log}_{10}(s) = 2.37$. Additionally, in each case we used a set of 20 different random maps $R(f_i, f_j)$ without modifying the average angular profile of the scattered light distribution $P(f_i, f_j)$ to investigate the effect of different distributions of opacities within the pupil for constant straylight level. The quality of retinal image was calculated using Eq. (6) and Eq. (9), and retinal image contrast (RIC) of sine wave grating was determined using Michelson formula:

$$RIC = \frac{I_{\max} - I_{\min}}{I_{\max} + I_{\min}} \text{ and } RIC_{AM-SC} = \frac{I_{AM-SC,\max} - I_{AM-SC,\min}}{I_{AM-SC,\max} + I_{AM-SC,\min}} \tag{10}$$

Finally, relative contrast difference (RCD) between blurred and compensated images was measured:

$$RCD = \frac{RIC_{AM-SC} - RIC}{RIC} \cdot 100\%. \tag{11}$$

2.3. Experimental setup

A single-pass optical system was developed to perform proof-of-concept study of the efficacy of AM-SC method in cataract eyes. The setup is schematically shown in Fig. 2.

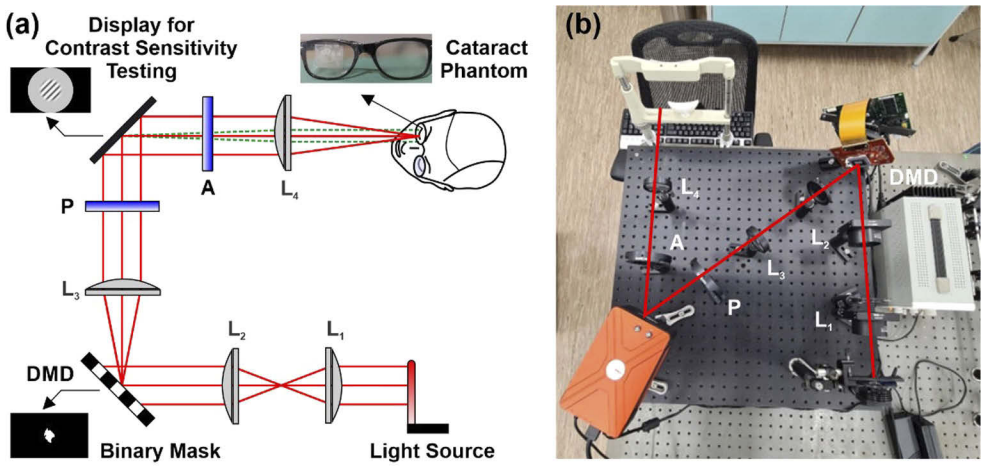

Fig. 2. (a) Experimental setup implementing AM-SC method equipped with a channel for contrast sensitivity testing. DMD – digital micro-mirror device, L1-L4 – lenses, P – polarizer and A – analyzer. (b) Photograph of the instrument.

A red light emitting diode (Ledox, Germany) with wavelength $\lambda = 625$ nm was used as a light source. The light beam was collimated by a pair of lenses L_1-L_2 (f_1, $f_2 = 75$ mm). The DMD (DMD DLP6500FQL; Texas Instruments Inc., USA) with an array of 1920×1080 micro-mirrors, each of 7.56 µm in size, was used as an amplitude modulator. The DMD plane was conjugated with the pupil plane via 4-f lens system made of lenses L_3 and L_4 (f_3, $f_4 = 250$ mm), which enabled spatial modulation of light amplitude entering the eye pupil (i.e. projection of binary amplitude masks at the pupil plane).The DMD was controlled by a software written in MatLab environment for the precise alignment of the mask at cataract phantom.

The stimuli to assess the contrast sensitivity were displayed by a reflective Liquid Crystal on Silicon Spatial Light Modulator (LCoS-SLM; EXULUS-HD1/M, Thorlabs Inc., USA) with an

Biomedical Optics EXPRESS

array of 1920×1080 pixels and pixel pitch 6.4 μm . This display was conjugated with the retinal plane of the subject's eye (indicated by green dashed lines in Fig. 2). LCoS-SLM was placed between two crossed linear polarizers (polarizer and analyzer) to use it as amplitude modulator and display stimuli of different spatial frequencies and contrast during contrast sensitivity tests.

A milky glue sample between two sheets of clear transparencies with random transparent areas was prepared as artificial light scatter model (cataract phantom), mimicking the scattering effects of cataract in healthy subjects. The cataract phantom was placed in spectacles which were worn by the subjects during the measurements of contrast sensitivity (see the photo in Fig. 2). The straylight parameter of cataract phantom was $\mathrm{Log}_{10}(s) = 2.37$ at 3 degrees, which was measured with optical integration method in a double-pass system [25]. In addition, the measured transport mean free path was 1.54 mm. The cataract phantom was also scanned with a swept-source OCT ($\lambda = 1.06$ μm, sweep rate 100 kHz, scan area 4.5×4.5 mm^2). *En face* projection of the OCT data of the phantom was used to generate the opacity maps. The latter was subject to thresholding, segmentation and inversion procedure to generate a binary mask, as described in Section 2.2.

2.4. Measurement of contrast sensitivity function

The contrast sensitivity testing was conducted with the aid of a software written in MatLab (Mathworks Ltd., USA) environment based on Psychtoolbox (psychtoolbox.org). Before the experiments, LCoS was calibrated for display application and later stimuli of spatial frequency of 1.5, 3, 6 and 12 CPD were displayed by using an adaptive psychometric method QUEST [26]. Four volunteers without any known ocular pathology (mean age 32.8 ± 3.3 years) participated in this study. The measurements were approved by the Ethical Commission at the University of Murcia and were in accordance to the tenets of the Declaration of Helsinki. The experiment was conducted in a dark room, and the subjects viewed the display monocularly through googles with cataract phantom. A chin rest permitted stabilization of the subject head to minimize the movements during the experiment. According to the measurement protocol, for each spatial frequency, the contrast threshold was firstly determined by an adjustment method. Then, a fine estimation of the contrast threshold was performed by the adaptive method QUEST [26].

The contrast sensitivity test was conducted twice for each subject, without and with amplitude modulation of the light beam to check how the AM-SC method works *in vivo*. DMD operated as a mirror during the first test (i.e. no modulation), whereas a binary masks was displayed on the DMD in the second test (i.e. with AM-SC method). Accordingly, the DMD operation permitted directing the light only through the transparent regions of cataract phantom.

3. Results

3.1. Simulation of intraocular scatter and operation of AM-SC method

Figure 3 shows the simulation results of the AM-SC method. The examples of synthetic opacity maps (phase maps from Eq. (1)) are presented in Fig. 3(a). Random distributions of opacities corresponding to nuclear cataract for two values of straylight parameter $\mathrm{Log}_{10}(s) = 1.75$ and $\mathrm{Log}_{10}(s) = 2.37$ are illustrated. Much finer grain texture can be observed when higher scattering is assumed. Based on opacity maps, we also generated binary masks. We would like to emphasize here that the opacified regions are zeroed out in binary mask so that the light would not pass through.

Later on, the opacity maps and binary masks were used to calculate the PSFs of the cataract eye before and after applying AM-SC method (Eqs. (5) and (8), respectively). Figure 3(b) shows the examples of the PSFs before and after the AM-SC technique implementation for the two above-mentioned amounts of straylight. The logarithmic intensity scale was used here to emphasize weaker signals. Higher lens opacification yields much higher degradation of the optical PSF so that the energy is distributed over a larger area. Moreover, the AM-SC method

Biomedical Optics EXPRESS

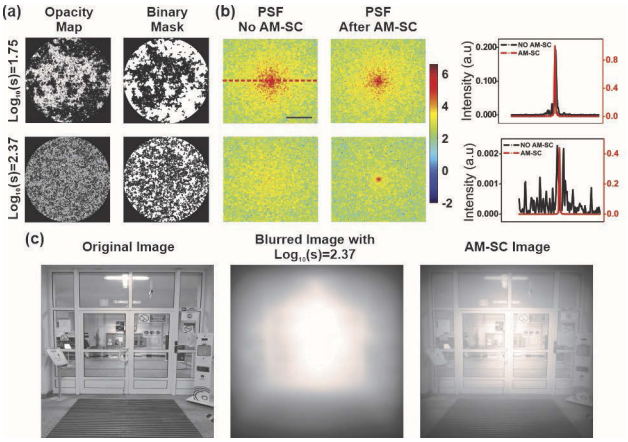

Fig. 3. Simulation of impact of intraocular scatter and AM-SC method on the retinal image in the cataract eye: (a) Opacity maps and corresponding binary masks for $\mathrm{Log}_{10}(s) = 1.75$ and $\mathrm{Log}_{10}(s) = 2.37$. (b) PSF with no compensation (PSF No AM-SC) and PSF after scatter compensation (PSF After AM-SC) with AM-SC method. Bar indicates 48 arcminutes. The normalized central intensity profiles along red dashed line plotted for before (No AM-SC; black) and after applying AM-SC method (After AM-SC; red). (c) Ground truth (original) image, retinal blurred image due to the simulated intraocular scattering $\mathrm{Log}_{10}(s) = 2.37$ and the retinal image after applying AM-SC method.

significantly improves the PSF for higher levels of scattering. This effect is due to the fact that in case of early-stage cataract ($\mathrm{Log}_{10}(s) = 1.75$), the scattering is relatively low and does not introduce much blurring, therefore its compensation is less effective. The improvement of PSF can be also visualized if one extracts central intensity profile from the PSF image. In this case, we used linear intensity scale, and the profiles were normalized to the PSF peak intensity value after compensation procedure was applied. The results show that 5- and even 200-fold improvement of central peak intensity can be achieved for $\mathrm{Log}_{10}(s)$ equals to 1.75 and 2.37, respectively.

We also applied the calculated PSFs to simulate the retinal images. Figure 3(c) illustrates exemplary ground truth (original) image, which was later blurred using a previously calculated PSF in the presence of scattering with the straylight parameter of $\mathrm{Log}_{10}(s) = 2.37$. It is a photo of the entrance to the faculty building. A complete loss of the details of the image of the entrance doors can be observed if the intraocular scattering effects due to advanced cataract are included. The retinal image with compensated scatter (AM-SC image) shows the improvement of the quality and allows to distinguish critical details enabling activity. It means that the vision quality could be partially restored although the AM-SC method does not reduce the scattering effects completely.

3.2. *Numerical simulations of AM-SC based contrast enhancement*

A set of 20 random phase matrices were generated to obtain sets of opacity maps for two values of straylight parameter $\mathrm{Log}_{10}(s) = 1.75$ and $\mathrm{Log}_{10}(s) = 2.37$. Then the images of sine-wave grating of the spatial frequency of 2, 6, 12 and 20 CPD, each with two modulation amplitude (contrast) values (100% and 50%), were prepared to serve as ground truth images. Those images were projected to synthetic cataract eyes, as described above. The retinal images were calculated with assumed levels of straylight without and after applying AM-SC method. The quality of the retinal images was quantified by measuring RIC (Eq. (10)). RIC change was expressed in percentage by calculating RCD. The results of the tests are presented in Fig. 4.

Biomedical Optics EXPRESS

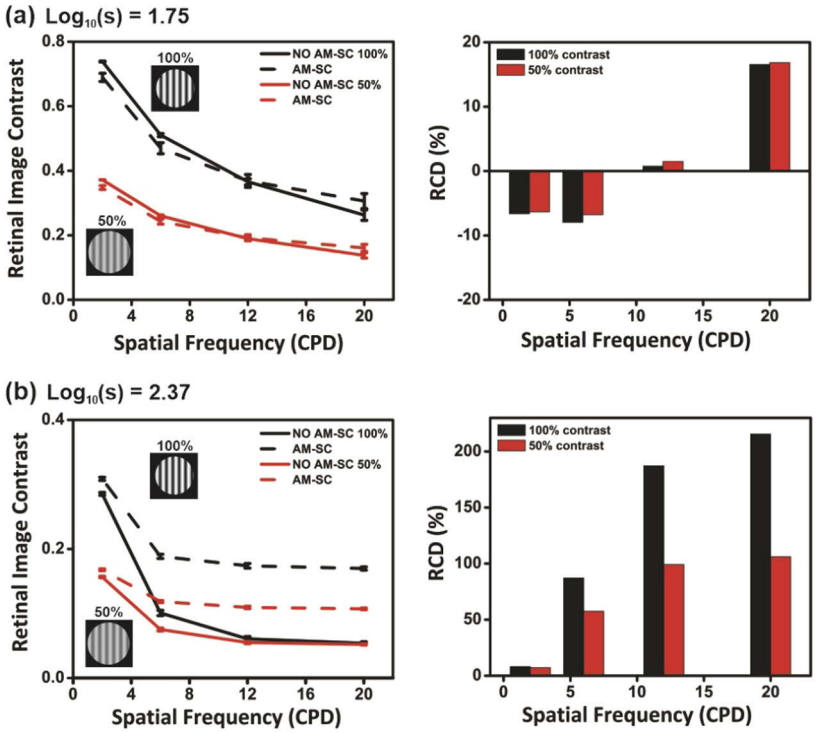

Fig. 4. Retinal image contrast (RIC) for sine-wave gratings of different spatial frequencies and contrast. Relative contrast difference (RCD) between retinal images after implementation of the AM-SC approach. Two levels of straylight parameter were used in calculations: (a), $Log_{10}(s) = 1.75$, and (b) $Log_{10}(s)$ 2. 37.

Generally, compared to early-stage cataract (lower $Log_{10}(s)$ value), RIC enhancement is more noticeable in advanced cataract when higher $Log_{10}(s)$ value was set. This is in agreement with the results shown in Fig. 3(a). No considerable improvement of retinal image quality is observed for $Log_{10}(s) = 1.75$. Actually, AM-SC method does not improve the retinal image when low spatial frequency grids are displayed, which is given by negative RCD values in Fig. 4(a). The improved image contrast as the result of scatter compensation is revealed for high spatial frequency of 20 CPD expressed by positive RCD values.

On the other hand, calculations for $Log_{10}(s) = 2.37$ show significant enhancement of retinal image contrast with the factor of 2× and 3× (i.e. RCD achieving 100% and 200%) even for higher spatial frequencies (Fig. 4(b)). In addition to that, higher improvement is observed for gratings with 100% contrast.

3.3. *In vivo measurements of contrast sensitivity function*

We conducted a pilot study to test the efficiency of AM-SC method in *in vivo* conditions. Contrast sensitivity tests were performed in four healthy volunteers with cataract phantom in front of their eyes. Accordingly, contrast sensitivity function (CSF) was measured without and with application of amplitude modulation (binary mask). The obtained CSFs for all subjects are presented in Fig. 5. Black solid curves represent CSFs without intraocular scattering compensation while red dashed curves demonstrate CSFs after AM-SC method.

Biomedical Optics EXPRESS

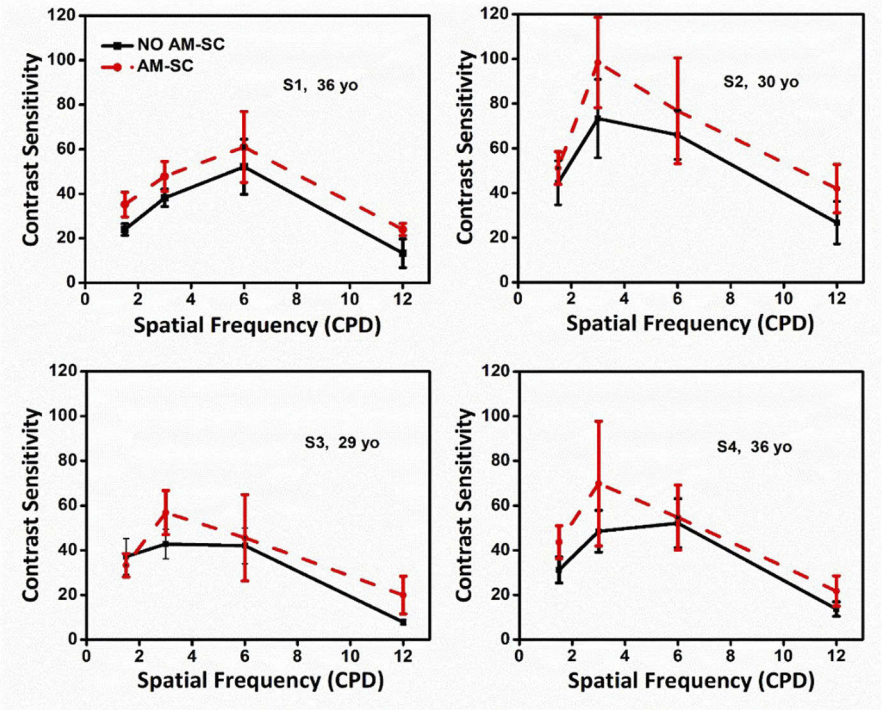

Fig. 5. Contrast sensitivity functions (CSFs) measured in four subjects (S1-S4) wearing the spectacles with cataract phantom. Black solid curves represent CFSs with no scatter compensation and red dashed curves represent CSFs after implementation of AM-SC method.

4. Discussion and conclusions

We demonstrated a novel method of intraocular scattering compensation with the aid of spatial modulation of light amplitude at the pupil plane. Experimentally, AM-SC applies recent advances in optical beam engineering to improve vision in patients with crystalline lens opacities. Similar approach of spatial light modulation has been used in the concept of stenopeic glasses (pinhole glasses), where pinhole perforations created a series of narrow beams for enhanced depth of focus.

Most of the previous efforts for scattering compensation in cataract eyes have been made by implementing either wavefront shaping methods or phase conjugation techniques. Research have also been done in preoperative prediction of visual performance in cataract patients, where the visual acuity chart has been projected at the retina in the form of narrow beams of light [27–29]. Recently Kavakli et al. proposed similar method of pupil steering via holographic display, to test the visual acuity of cataract patients and to predict postoperative vision [30].

The AM-SC method depends on the prior knowledge of the spatial distribution of opacities in the cataract lens. Therefore, an earlier imaging procedure is required to obtain the opacity projection map within the eye pupil area. A binary mask generated based on such opacity map can facilitate the light to avoid interaction with the opacities. The *in vivo* measurements were completed by simulating the cataract with a phantom but future experiments should involve cataract patients. Relevant simulations were performed that enabled correction of adverse effects of nuclear cataract (from early to advanced stage) on visual quality. The simulated PSF of the cataract eye after application of the AM-SC method showed improved light focusing in comparison to the uncompensated case, and, what is more, the AM-SC technique appeared

Biomedical Optics EXPRESS

more efficient in case of more advanced cataract, although the scattering itself has not been fully suppressed. Like the PSF of any optical instrument, the retinal PSF relates directly to the quality of the image formed at the retina. Therefore, improvement of the retinal PSF should also enhance the quality of vision by reducing the blur and increasing the image contrast. This contrast improvement was also investigated quantitatively in our studies by calculating the so-called Michelson contrast of retinal images in a sine wave grating test. The mentioned grating test was simulated for high and low contrast conditions and it revealed that the AM-SC method indeed improves the contrast at the retinal plane, especially in the case of high spatial frequency information.

Moreover, contrast sensitivity testing by an adaptive method, QUEST, was conducted in *in vivo*, on four healthy subjects with simulated monocular cataract phantom in a single pass system. Contrast sensitivity examination demonstrated an increase in contrast sensitivity with the AM-SC method being applied, which was consistent for all the investigated subjects, for high spatial frequencies. The experimental setup that was proposed to test the validity of the AM-SC technique, can also be used to inspect visual acuity of cataract patients before a potential operation, to estimate the postoperative visual performance of these patients.

There are some factors that limit the performance of the AM-SC method. Firstly, it is worth to note that in the discussed technique the light is only allowed to pass through transparent parts of the cataract lens and is blocked before reaching the opacities. Therefore one should expect lower total light intensity at the pupil plane of the eye, which may need consideration, especially in low light conditions. Secondly, the proposed method cannot be too effective in case of dense opacification of crystalline lens, where there is no transparency at all. Thirdly, the movements of the examined pupil can also result in displacement of the projected mask image at the pupil plane, which in consequence will lead to image contrast reduction at the retinal plane. This phenomenon, however, can be addressed by monitoring eye globe movements and a careful digital control of the displayed mask, which would need to be correlated with the pupil movements.

To conclude, we developed and tested a method for compensation of intraocular optical scattering via spatial light amplitude modulation within the eye pupil area of partially opacified crystalline lens. This technique may allow to minimize the impact of the opacifications within the lens on the retinal image quality. The performance of the method was studied by numerical simulations of point spread functions and retinal images, corresponding to the presence of different amount of stray light. The AM-SC method has the capability to improve the visual quality in cataract patients, as shown by the measurements of CSFs in the human eyes *in vivo* with artificial light scatter model. The proposed method can be used for the postoperative vision prediction for cataract patients and also it can facilitate the patients to have realistic expectation regarding the outcome of cataract surgery. The proposed method can be clinically implemented with the use of virtual reality technology [31]. Future research activities will focus on assessing the operation of the AM-SC method in cataract patients.

Funding. Fundacja na rzecz Nauki Polskiej (POIR.04.04.00-00-5C9B/17-00); Agencia Estatal de Investigación (PID2019-105684RB-I00/AEI/10.13039/501100011033); Fundación Séneca (19897/GERM/15); Horizon 2020 Framework Programme (897300).

Disclosures. The authors declare no conflicts of interest.

Data availability. Data underlying the results presented in this paper are available in Ref. [32].

References

1. M. Ljungberg and P. H. Pretorius, "SPECT/CT: an update on technological developments and clinical applications," Br. J. Radiol. **91**(1081), 20160402 (2018).
2. C. C. Watson, "New, faster, image-based scatter correction for 3D PET," IEEE Trans. Nucl. Sci. **47**(4), 1587–1594 (2000).
3. R. Horstmeyer, H. Ruan, and C. Yang, "Guidestar-assisted wavefront-shaping methods for focusing light into biological tissue," Nat. Photonics **9**(9), 563–571 (2015).

Biomedical Optics EXPRESS

4. P. Lysakovski, A. Ferrari, T. Tessonnier, J. Besuglow, B. Kopp, S. Mein, T. Haberer, J. Debus, and A. Mairani, "Development and benchmarking of a Monte Carlo dose engine for proton radiation therapy," Front. Phys. **9**, 741453 (2021).
5. M. A. May, N. Barre, K. K. Kummer, M. Kress, M. Ritsch-Marte, and A. Jesacher, "Fast holographic scattering compensation for deep tissue biological imaging," Nat. Commun. **12**(1), 4340 (2021).
6. I. N. Papadopoulos, J. S. Jouhanneau, J. F. A. Poulet, and B. Judkewitz, "Scattering compensation by focus scanning holographic aberration probing (F-SHARP)," Nat. Photonics **11**(2), 116–123 (2017).
7. M. Rosenfeld, G. Weinberg, D. Doktofsky, Y. Z. Li, L. Tian, and O. Katz, "Acousto-optic ptychography," Optica **8**(6), 936–943 (2021).
8. A. K. Singh, D. N. Naik, G. Pedrini, M. Takeda, and W. Osten, "Exploiting scattering media for exploring 3D objects," Light: Sci. Appl. **6**(2), e16219 (2017).
9. P. Artal, "Optics of the eye and its impact in vision: a tutorial," Adv. Opt. Photonics **6**(3), 340–367 (2014).
10. R. Michael and A. J. Bron, "The ageing lens and cataract: a model of normal and pathological ageing," Phil. Trans. R. Soc. B **366**(1568), 1278–1292 (2011).
11. H. E. Gali, R. Sella, and N. A. Afshari, "Cataract grading systems: a review of past and present," Curr. Opin. Ophthalmol. **30**(1), 13–18 (2019).
12. P. Artal, A. Benito, G. M. Perez, E. Alcon, A. De Casas, J. Pujol, and J. M. Marin, "An objective scatter index based on double-pass retinal images of a point source to classify cataracts," PLoS One **6**(2), e16823 (2011).
13. A. de Castro, A. Benito, S. Manzanera, J. Mompean, B. Canizares, D. Martinez, J. M. Marin, I. Grulkowski, and P. Artal, "Three-dimensional cataract crystalline lens imaging with swept-source optical coherence tomography," Invest. Ophthalmol. Vis. Sci. **59**(2), 897–903 (2018).
14. L. Franssen, J. E. Coppens, and T. J. van den Berg, "Compensation comparison method for assessment of retinal straylight," Invest. Ophthalmol. Vis. Sci. **47**(2), 768–776 (2006).
15. I. Grulkowski, S. Manzanera, L. Cwiklinski, J. Mompean, A. de Castro, J. M. Marin, and P. Artal, "Volumetric macro- and micro-scale assessment of crystalline lens opacities in cataract patients using long-depth-range swept source optical coherence tomography," Biomed. Opt. Express **9**(8), 3821–3833 (2018).
16. D. Christaras, H. Ginis, A. Pennos, and P. Artal, "Intraocular scattering compensation in retinal imaging," Biomed. Opt. Express **7**(10), 3996–4006 (2016).
17. A. Arias and P. Artal, "Wavefront-shaping-based correction of optically simulated cataracts," Optica **7**(1), 22–27 (2020).
18. S. Marcos, E. Martinez-Enriquez, M. Vinas, A. de Castro, C. Dorronsoro, S. P. Bang, G. Yoon, and P. Artal, "Simulating outcomes of cataract surgery: important advances in ophthalmology," Annu. Rev. Biomed. Eng. **23**(1), 277–306 (2021).
19. E. Chan, O. A. R. Mahroo, and D. J. Spalton, "Complications of cataract surgery," Clin. Exp. Optom. **93**(6), 379–389 (2010).
20. D. Miller, J. L. Zuckerman, and G. O. Reynolds, "Phase aberration balancing of cataracts using holography," Exp. Eye Res. **15**(2), 157–160 (1973).
21. Y. Liu, Y. C. Shen, H. W. Ruan, F. L. Brodie, T. T. W. Wong, C. H. Yang, and L. H. V. Wang, "Time-reversed ultrasonically encoded optical focusing through highly scattering ex vivo human cataractous lenses," J. Biomed. Opt. **23**(01), 1–4 (2018).
22. A. M. Paniagua-Díaz, A. Jiménez-Villar, I. Grulkowski, and P. Artal, "Double-pass wavefront shaping for scatter correction in a cataract's model," Opt. Express **29**(25), 42208–42214 (2021).
23. A. Arias, H. Ginis, and P. Artal, "Light scattering in the human eye modelled as random phase perturbations," Biomed. Opt. Express **9**(6), 2664–2670 (2018).
24. B. L. C. J. J. Vos, H.-W. Bodmann, E. Colombo, T. Takeuchi, and T. J. T. P. van den Berg, "CIE equations for disability glare," CIE Publication **146**, 2002 (2002).
25. H. Ginis, O. Sahin, A. Pennos, and P. Artal, "Compact optical integration instrument to measure intraocular straylight," Biomed. Opt. Express **5**(9), 3036–3041 (2014).
26. A. B. Watson and D. G. Pelli, "Quest - a Bayesian adaptive psychometric method," Percept. Psychophys. **33**(2), 113–120 (1983).
27. S. A. Melki, A. Safar, J. Martin, A. Ivanova, and M. Adi, "Potential acuity pinhole - A simple method to measure potential visual acuity in patients with cataracts, comparison to potential acuity meter," Ophthalmology **106**(7), 1262–1267 (1999).
28. J. S. Minkowski, M. Palese, and D. L. Guyton, "Potential acuity meter using a minute aerial pinhole aperture," Ophthalmology **90**(11), 1360–1368 (1983).
29. M. Vianya-Estopa, W. A. Douthwaite, C. L. Funnell, and D. B. Elliott, "Clinician versus potential acuity test predictions of visual outcome after cataract surgery," Optometry **80**(8), 447–453 (2009).
30. G. A. K. Kavakli, E. Ulusoy, C. Kesim, M. Hasanreisoglu, A. Sahin, and H. Urey, "Pupil steering holographic display for pre-operative vision screening of cataracts," J. Biomed. Opt. **12**(12), 7752–7764 (2021).
31. G. Aydindogan, K. Kavakli, A. Sahin, P. Artal, and H. Urey, "Applications of augmented reality in ophthalmology [Invited]," Biomed. Opt. Express **12**(1), 511–538 (2021).

Biomedical Optics EXPRESS

32. S. Panezai, A. Jiménez-Villar, A. M. Paniagua-Díaz, A. Arias, G. Gondek, S. Manzanera, P. Artal, and I. Grulkowski, "Intraocular scatter compensation with spatial light amplitude modulation for improved vision in simulated cataractous eyes: dataset'," Zenodo, 2021, https://zenodo.org/record/5792882#.YcBTU2DMI2w.

155.54.207.227 {ts '2022-03-17 04:30:15'}